VOID FORMATION DURING PREFORM IMPREGNATION IN LIQUID COMPOSITE MOLDING PROCESSES

C. DeValve and R. Pitchumani

Advanced Materials and Technologies Laboratory, Department of Mechanical Engineering, Virginia Polytechnic Institute and State University, Blacksburg, Virginia 24061-0238, USA, pitchu@vt.edu

ABSTRACT: It is well known that air entrapment during the mold filling stage of liquid composite molding processes leads to defects in the resulting composite, such as discontinuous material properties and failure zones which need to be eliminated or reduced. To this end, an accurate prediction of local air entrapment locations during processing is necessary. This study presents a detailed numerical simulation of the coupled effects of the unsaturated macro-scale flow of the advancing resin flow front around individual fiber bundles combined with the simultaneous micro-scale flow through the fiber bundles in a plain weave preform geometry. The primary goal is to develop a predictive paradigm for the location and relative size of the resulting voids as a function of the permeability and process parameters. Based on the numerical simulation results, strategies for void-free mold filling are presented and discussed.

KEYWORDS: void formation, liquid composite molding, resin transfer molding, vacuum assisted resin transfer molding, computational simulations, process control

INTRODUCTION

The selection of fiber weave in the preform, mold complexity, resin type, and imposed pressure gradient on the fiber layup all affect the development of the resin flow field through the fiber tows during liquid composite molding, and consequently, the entrapment of air voids in the resulting cured composite material. The flow through fibrous preforms is fundamentally governed by the preform permeability, which is a measure of the resistance offered to the flow by the porous structure of the preform. Several studies are reported in the literature on relating the transverse and longitudinal permeability to the porosity of fiber bundles for idealized rectangular and staggered packing arrangements of fibers in the tow bundles [1,2 for example]. A full review of experiments and theoretical predictions of low Reynolds number flow through fibrous porous media detailing porosity-permeability relationships was compiled by Jackson and James [3]. Several techniques have been explored in the literature to model the void entrapment in liquid molding processes. The lattice Boltzmann method was used by Spaid and Phelan [4] to

simulate flow through square-packed fiber tows. Parnas [5] used Darcy's law to develop a model of air entrapment in a fiber tow with resin permeating the fiber cross-section radially inward. Foley and Gillespie [6] further extended the model proposed by Parnas [5] with a similar approach and studied the effect of individual fiber diameter and fiber bundle count on the resulting size of the entrapped air void within the fiber tow. A control volume approach to void formation prediction was investigated by Jinlian, et al. [7] and applied to a two-dimensional unit cell cross-section of various multi-layer woven fabrics, where the resulting simulations were able to predict voids in the low permeability regions in the fiber architecture.

The studies in the literature have focused primarily on two-dimensional geometry of the fiber bundles, whereas the flow in actual processing is three-dimensional. Toward prediction of void entrapment in realistic preform micro-geometries, the present study uses numerical simulation to investigate permeating resin flow through a three-dimensional unit cell of plain weave fiber preform. Considering unsaturated resin flow, the resulting evolution of the macro- and micro-scale resin flow progression is studied for a range of tow permeabilities and driving pressure gradients. Based on the results, conditions that lead to void-free fill are identified.

NUMERICAL MODEL

Figure 1(a) shows the representative volume element of a plain weave preform architecture in which each fiber bundle consisting of numerous individual fiber tows was modeled as a porous medium with a defined porosity-permeability relationship. The cross-running fiber tow was centered with respect to the inlet and outlet faces of the unit cell, and symmetrical boundary conditions were applied on the left and right faces of the unit cell as well as on the top and bottom faces. The weave of the fiber bundle was shaped as a sinusoidal function and the cross section of the bundle was defined to be lenticular in shape. A permeability tensor was defined along the curvature of the fiber bundle based on projecting the longitudinal and transverse permeability values onto the local axis of the fiber bundle throughout the unit cell.

The incompressible Brinkman equation [1] was used to model both the resin and air flow through the porous media (fiber bundle), given as:

$$\frac{\rho}{\varepsilon}\frac{\partial \boldsymbol{u}}{\partial t} + \frac{\mu}{\kappa}\boldsymbol{u} = -\nabla p + \frac{\mu}{\varepsilon}(\nabla^2 \boldsymbol{u}) \tag{1}$$

where ρ is the density, ε is the porosity, $\boldsymbol{u}$ is the velocity vector, μ is the viscosity, κ is the permeability, and p is pressure. The phase field method was used to keep track of the resin-air interface in the fiber tow by solving the following equation throughout the flow field:

$$\frac{\partial \varphi}{\partial t} + \boldsymbol{u} \cdot \nabla \varphi = -\nabla \cdot \frac{\gamma \lambda}{\sigma^2} \nabla (\nabla \cdot \sigma^2 \nabla \varphi - (\varphi^2 - 1)\varphi) \tag{2}$$

Here φ is the dimensionless phase field parameter (forced to 1 for air or -1 for the resin except along the thin transitional interface region), γ is the mobility parameter which controls the relaxation time, λ is the mixing energy density, and σ is the capillary width that scales with the thickness of the thin interface region. Equations (1)–(2) were solved using the commercially available software COMSOL version 3.5a.
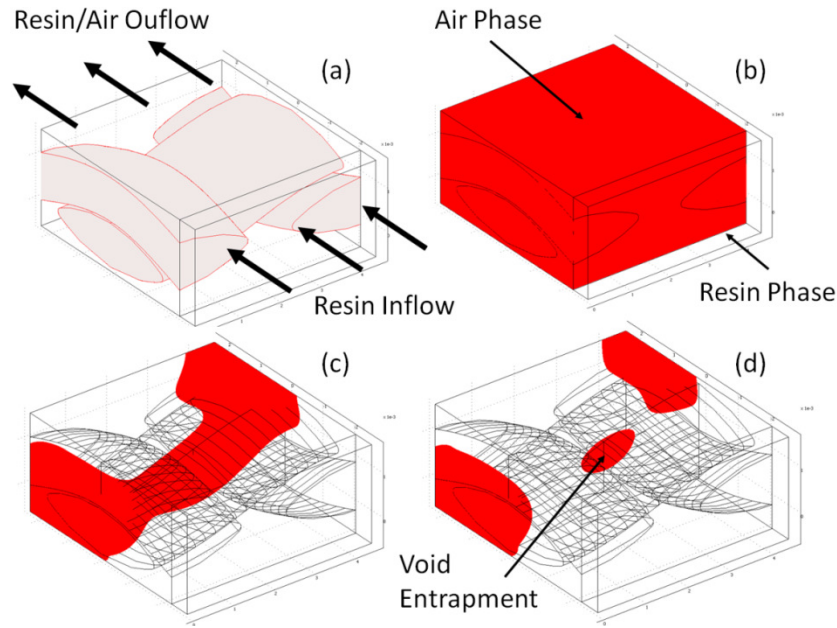
Figure 1: (a) The plain weave preform architecture unit cell used in the numerical simulations and (b) an initially air-filled (shaded region) unit cell with uniform advancing resin (unshaded region) at t = 0 s, (c) t = 0.02 s, and (d) t = 0.04 s, where the entrapment of an air-filled void is evident in the cross-running fiber bundle

The resin properties were chosen to be those of Shell EPON Resin 828 with Shell Epicure 3274 catalyst and the tow bundle dimensions were based on WR10/3010 plain weave fabric from Owens Corning. Considering the fiber arrangement in the bundle to be idealized as square or hexagonal packing, the transverse permeability of the fiber bundles was evaluated as a function of the bundle porosity and fiber diameter and validated against the results of Bruschke and Advani [2]. An analytical expression for the longitudinal permeability-porosity relationship was developed by modeling the flow through a two-dimensional cross-section of the particular packed fiber arrangement as an equivalent flow through a pipe with the hydraulic diameter corresponding to the unit cell of this geometry. The average flow rate longitudinally through the two-dimensional cross-section was related to the pressure gradient, permeability, and the viscosity using a one-dimensional Darcy's Law, from which a porosity-permeability relationship was established and validated against results summarized by Jackson and James [3].

RESULTS AND DISCUSSION

The unsaturated flow through the plain weave unfilled geometry was simulated under porosity conditions approaching the packing limit with the assumption of both square and hexagonal packing of the individual fiber tows within each fiber bundle. The results of permeating resin flow through the plain weave fabric architecture are presented in Figures 1(b)–(d) for a longitudinal to transverse permeability ratio of $2x10^4$ and a pressure gradient of 1778 kPa/m. Note that the air phase is represented by the shaded region(s) in Figure 1 so as to best visualize the presence of entrapped air-voids. The remaining unshaded region(s) within the unit
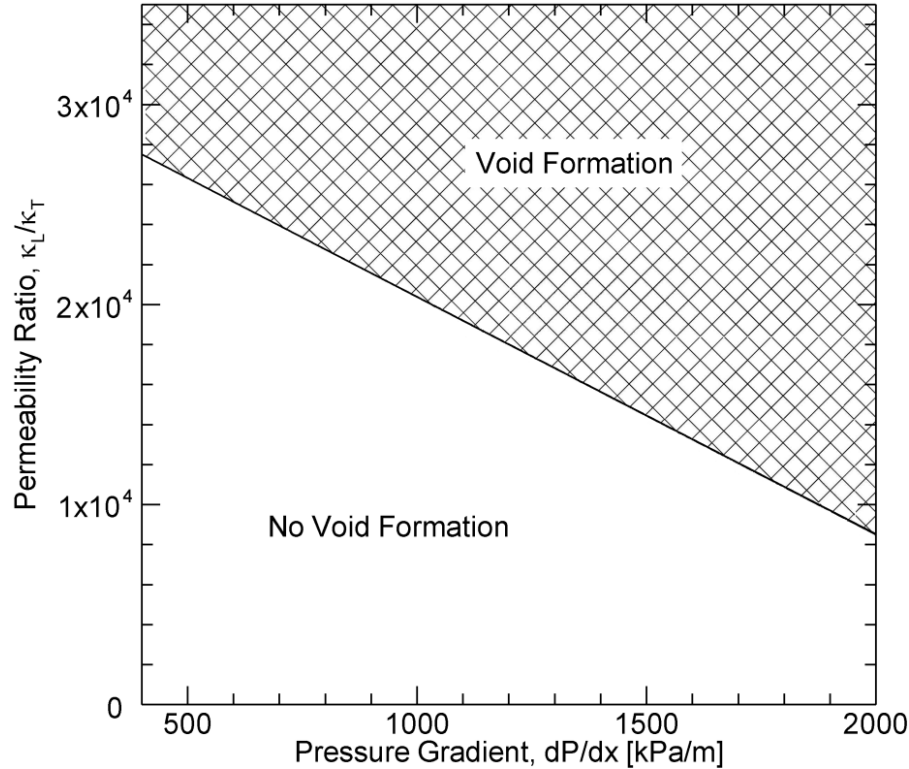
Figure 2: Mapping of permeability ratio and pressure gradient combinations that lead to void-free mold filling (unhatched region) and filling with void entrapment (hatched region)

cell represents the resin phase of the numerical simulation. Figure 1(b) presents the initial unit cell configuration, with a uniform inlet resin velocity profile at the air-resin interface. The penetrating resin flow at t = 0.02 s is shown in Figure 1(c), where the resin has partially filled the unit cell and a significant amount of air remains within the cross-running fiber tow. Figure 1(d) presents the simulation at t = 0.04 s, where the resin has almost completely filled the unit cell and an entrapped air void remains near the center of the cross-running fiber tow.

Systematic studies were conducted by varying the longitudinal to transverse permeability ratio and the pressure gradient to explore a range of preform micro-architecture and processing condition scenarios. Each simulation was analyzed for void entrapment and initial void size as the resin permeated the unit cell. Figure 2 presents the numerical simulation results as a map of the longitudinal to transverse permeability ratio and pressure gradient combinations that lead to entrapped voids or otherwise. It is evident from the results that void formation occurs at both high pressure gradients and high permeability ratios. For a given permeability ratio, as the pressure gradient is increased, the likelihood of void formation increases as the macro-scale resin flow is forced quickly around the fiber bundles relative to the micro-scale flow through the fiber bundles, resulting in void formation within the fiber bundle. Additionally, for a given pressure gradient, as the permeability ratio is increased the micro-scale flow is directed longitudinally through the fiber bundle at a much higher rate in comparison to the flow transverse to the fiber tows, resulting in air entrapment within the fiber bundle oriented transverse to the resin flow direction. Furthermore, although not presented in Figure 2, the numerical simulation results show that the initial size of the entrapped void increases with increase in the longitudinal to transverse

permeability ratio and in the pressure gradient. Figure 2 provides for selection of line injection parameters for a given plain weave geometry (with its corresponding longitudinal to transverse permeability ratio), so as to attain void-free processing.

CONCLUSIONS

A numerical model of the unsaturated resin infiltration through a three-dimensional plain weave fiber preform geometry was presented and analyzed by varying the permeability ratio and pressure gradient imposed on the flow with the aim of predicting the presence and initial size of entrapped air voids within the fiber tows. It was found that both high pressure gradients and high longitudinal to transverse permeability ratios result in the onset of void formation and increase in the initial void size. Ongoing research will be focused on studying the effect of different fiber weave architectures, nesting fiber bundles from sandwiched mat layers, and down-stream flow evolution (multiple unit cells) on the resulting void formation within the fiber tows.

ACKNOWLEDGEMENTS

REFERENCES

1. S. G. Advani, "Flow and Rheology in Polymer Composites Manufacturing", Elsevier Science B.V., The Netherlands, (1994).

2. M. V. Bruschke and S. G. Advani, "Flow of Generalized Newtonian Fluids Across a Periodic Array of Cylinders", *Journal of Rheology*, Vol. 37, no. 3, pp. 479–498 (1993).

3. G. W. Jackson and D. F. James, "The Permeability of Fibrous Porous Media", *Canadian Journal of Chemical Engineering*, Vol. 64, pp. 364–374 (1986).

4. M. A. A. Spaid and F. R. Phelan Jr., "Modeling Void Formation Dynamics in Fibrous Porous Media with the Lattice Boltzmann Method", *Composites Part A: Applied Science and Manufacturing*, Vol. 29A, pp. 749–755 (1998).

5. R. S. Parnas, "Liquid Composite Molding", Hanser Gardner Publications, Ohio, (2000).

6. M. E. Foley and J. W. Gillespie Jr., "Modeling the Effect of Fiber Diameter and Fiber Bundle Count on Tow Impregnation During Liquid Molding Processes" *Journal of Composite Materials*, Vol. 39, no. 12, pp. 1045–1065 (2005).

7. H. Jinlian, L. Yi, and S. Xueming, "Study on Void Formation in Multi-Layer Woven Fabrics", *Composites Part A: Applied Science and Manufacturing*, Vol. 35, pp. 595–603 (2004).